J Nanopart Res (2013) 15:1554
DOI 10.1007/s11051-013-1554-0

RESEARCH PAPER

Enhanced microwave shielding and mechanical properties of high loading MWCNT–epoxy composites

B. P. Singh · Prasanta · Veena Choudhary · Parveen Saini · Shailaja Pande · V. N. Singh · R. B. Mathur

Received: 17 September 2012 / Accepted: 28 February 2013 / Published online: 14 March 2013

Abstract Dispersion of high loading of carbon nanotubes (CNTs) in epoxy resin is a challenging task for the development of efficient and thin electromagnetic interference (EMI) shielding materials. Up to 20 wt% of multiwalled carbon nanotubes (MWCNTs) loading in the composite was achieved by forming CNT prepreg in the epoxy resin as a first step. These prepreg laminates were then compression molded to form composites which resulted in EMI shielding effectiveness of −19 dB for 0.35 mm thick film and −60 dB at for 1.75 mm thick composites in the X-band (8.2–12.4 GHz). One of the reasons for such high shielding is attributed to the high electrical conductivity of the order of 9 S cm^{-1} achieved in these composites which is at least an order of magnitude higher than previously reported results at this loading. In addition, an improvement of 40 % in the tensile strength over the neat resin value is observed. Thermal conductivity of the MWCNTs–epoxy composite reached 2.18 W/mK as compared to only 0.14 W/mK for cured epoxy.

Keywords Carbon nanotubes · Nanocomposites · Electrical properties · Mechanical properties · Microwave shielding

B. P. Singh (✉) · Prasanta · S. Pande · R. B. Mathur (✉)
Physics and Engineering of Carbon, Division of Materials Physics and Engineering, CSIR-National Physical Laboratory, New Delhi 110012, India
e-mail: bps@mail.nplindia.org; bps@mail.nplindia.ernet.in

R. B. Mathur
e-mail: rbmathur@mail.nplindia.org

V. Choudhary
Centre for Polymer Science and Engineering, Indian Institute of Technology Delhi, Delhi 110016, India

P. Saini
Polymeric and Soft Materials Section, CSIR-National Physical Laboratory, New Delhi 110012, India

V. N. Singh
Electron and Ion Microscopy Section, CSIR-National Physical Laboratory, New Delhi 110012, India

Introduction

Electromagnetic interference (EMI) shielding of radio frequency radiation continues to be a serious concern in modern society due to increasing use of commercial, military and electronic devices. In order to protect the society from these harmful radiations, various shielding materials have been used in past. Conventional metals were the first choice for researchers and industrialists till the last few decades. Compared to conventional metal-based EMI shielding materials, electrically conducting polymer composites have gained popularity recently because of their light weight, resistance to corrosion, flexibility, and processing advantages (Liu et al. 2007). The EMI shielding effectiveness (SE) of a composite material

depends mainly on the filler's intrinsic conductivity, dielectric constant and aspect ratio (Li et al. 2006). The high conductivity, small diameter, high aspect ratio and superior mechanical properties of carbon nanotubes (CNTs) make them an excellent choice to be used as conductive composites for high performance EMI shielding materials. EMI shielding in the range of 8.2–12.4 GHz (X-band) is very important for military and commercial applications. Doppler, weather radar, TV picture transmission, and telephone microwave relay systems lie in this frequency range (Huang et al. 2007). Recently, several studies have been reported on CNTs reinforced thermoplastic polymer composites as effective and light weight EMI shielding materials in X-band. These include poly(methyl methacrylate) (PMMA) (Kim et al. 2004; Mathur et al. 2008b; Pande et al. 2009; Yuen et al. 2008), polystyrene(PS) (Mathur et al. 2008b; Yang & Gupta, 2005) polypropylene (PP) (Al-Saleh and Sundararaj 2009), polyurethane (PU) (Liu et al. 2007), polyvinylidene fluoride (PVDF) (Eswaraiah et al. 2011), poly(trimethyene terephthalate) (Gupta and Choudhary 2011), polyacrylate (Li et al. 2008), styrene acrylic emulsion (Li et al. 2010), cellulose triacetate (Basavaraja et al. 2011), ethylene vinyl acetate (EVA) (Das and Maiti 2008), reactive ethylene terepolymer (RET) (Park et al. 2010), and polycarbonate (PC) (Arjmand et al. 2011).

Epoxy resins are well established as thermosetting matrices for advanced structural composites, displaying a series of promising characteristics for a wide range of applications owing to their excellent mechanical properties, low cost, ease of processing, good adhesion to many substrates, and good chemical resistance (Garg et al. 2011). Several fibrous reinforcements e.g., carbon fibers, glass fibers, and aramid fiber (Kevlar fibers) etc. (Morais and Godfroid 2003) have been used with epoxy resin as matrix in producing structurally strong composite materials for commercial applications such as in aerospace industry. It suggests that CNT reinforced epoxy composites can also be a structurally strong EMI shielding material. Few studies have been reported on CNT–epoxy composites as EMI shielding material. Huang et al. (2007) have reported EMI-SE of 18 dB for composite with 15 wt% small single-walled carbon nanotubes (SWCNTs) and 23–28 dB for composite with 15 wt% long SWCNTs in the frequency band of 8–12.4 GHz. Li et al. (2006) observed the SE of 49.2 dB at 10 MHz for composite with 15 wt% long CNTs. It was reported that at higher frequencies (1 GHz), composites exhibited SE of 20 dB for both composites with 10 and 15 wt% SWCNT loadings. There are very few reports on CNT–epoxy composites for EMI shielding in X-band. Thus, there is a need to explore structurally strong MWCNT–epoxy composites for EMI shielding effectiveness in X-band. The reason behind fewer reports in CNT–epoxy composites is the need for high loading of CNTs required for high conductivity and EMI shielding. To improve the electrical conductivity and mechanical properties, higher loading of CNTs in EMI shielding composites is required (Park et al. 2009). But dispersion of high loading of CNTs in epoxy resin is difficult due to formation of agglomerates by the conventional techniques. However, epoxy composites synthesized using the conventional methods generally have low CNT contents. It has been reported that beyond 0.6 wt% of MWCNT, CNT tend to agglomerate (Yang et al. 2009) resulting in poor bending strength and modulus of the composites.

It is therefore important to develop a technique to incorporate higher CNT loading in epoxy resin without sacrificing their mechanical properties. Recently, several methods have been developed for fabricating CNT/polymer composites with high CNT loadings. One such technique is mechanical densification technique where vertically aligned CNTs were densified by the capillary-induced wetting with epoxy resin (Wardle et al. 2008).This technique is limited by the sample size. In another technique, a filtration system was used to impregnate the epoxy resin into CNT bucky paper (Gou 2006; Wang et al. 2004). However, it was very difficult to completely impregnate the bucky paper with epoxy resin. Recently, Feng et al. (2010) has reported a mixed curing-assisted layer-by-layer method to synthesize MWCNT/epoxy composite film with high CNT loading from ~15 to ~36 wt%. The electrical conductivity of the composites showed a value of 0.12 S/cm. However, the mechanical properties of the composites were not reported. In another study by Feng et al (2011), up to ~39.1 wt% SWCNT–epoxy composites were fabricated having enhanced mechanical properties. However, in all the above studies, EMI shielding effectiveness of these composites has not been reported. In one of our previous study, we observe that it was not possible to disperse more than 0.5 % by weight of MWCNT in the epoxy resin due to

agglomeration of the tubes at higher loadings (Garg et al. 2011). These small loadings did not contribute significantly toward EMI shielding despite having high electrical conductivity of these tubes. Therefore, a new technique was used to increase the loading of MWCNT by coating the individual nanotube with epoxy resin in the form of prepreg. We report here the electrical, mechanical, thermal, and EMI shielding of such composites. Scanning electron microscope (SEM) and high resolution transmission electron microscope (HRTEM) are used to investigate morphological and microstructural properties to establish a correlation between microstructure and mechanical/electrical properties of the composites.

Experimental

Materials

Di-glycidyl ether of bisphenol A (DGEBA) type epoxy resin (LY-556, Huntsman Co. Inc.) was used as the matrix material. Aradur (HY5200, Huntsman Co. Inc.) was used as a curing agent. MWCNTs were synthesized using toluene as a carbon source and ferrocene as catalyst precursor in a CVD set-up established in the laboratory (Mathur et al. 2008a). The MWCNTs produced were 10–70 nm in diameter and ~200-μm in length (Singh et al. 2011). These were 90 % pure with 10 wt% of Fe catalyst.

Fabrication of MWCNT–epoxy composites

Fabrication process of MWCNTs–epoxy composites is depicted schematically in Fig. 1. The different amounts of as-grown MWCNTs (a) was dispersed in acetone for 2 h in ultrasonic bath for opening the bundles (b).The epoxy resin (c) was diluted with acetone to reduce the viscosity of the resin (d).The dispersed MWCNTs were added in diluted epoxy resin and magnetically stirred for 24 h to obtain a uniform dispersion (e).The curing agent was added in the ratio of 100 (epoxy) : 23 (hardener) by weight in the dispersed material and magnetically stirred for 30 min (f). The dispersed MWCNTs in epoxy resin were filtered in a specially designed filtration unit (g) to form a film of epoxy impregnated MWCNT and dried at 80 °C for 2 h to form MWCNT–epoxy prepreg (h). The prepreg was compression molded in hydraulic press between two plates at 80 °C followed by curing under press at 150 °C for 4 h. The resultant composite paper containing different percentage of CNTs were obtained in the form of a uniform circular disk of 10 cm dia. This compression molded cured film was cut into the desired shape (i) for further testing. For the preparation of composite block (k) from these prepreg, the prepreg papers were cut into the shape of 60×20 mm^2 size (j) and placed in a three piece mold for compression molding in hydraulic press.

Characterization

The fractured surface of MWCNT–epoxy composite samples was analyzed by SEM (Leo model: S-440). HRTEM studies of MWCNTs were carried out using Technai G20-stwin, 300 kV instrument. The MWCNT content in epoxy matrix was determined using a thermogravimetric analyzer (TGA) (Mettler Toledo TGA/SDTA 851 e). The test was performed between 30 and 600 °C at a heating rate of 10 °C/min under nitrogen with a flow rate of 50 cc/min. Thermal diffusivity of the composite samples was measured using a Nflash Line 3000 (Anter make) system using a standard test method for thermal diffusivity by flash technique. The thermal conductivity of the samples was determined by measuring the specific heat of the sample on the same instrument. The measurement is based on ASTM-E-1461. The tensile strength and Young's modulus of pure epoxy and MWCNT–epoxy composite film was measured using an Instron machine model 4411. The composite films were cut into standard dog bone shape (Mathur et al. 2008b; Allaoui et al. 2002) using ASTM D638. A special die-punch was used for the purpose. The gauge length and width of the test sample were 30 and 6 mm, respectively. The cross–head speed was maintained at 0.5 mm/min. The electrical conductivity of composite films (60 mm × 20 mm × 0.35 mm) was measured by d.c four probe contact method (Singh et al. 2011; Singh et al. 2008) using a Keithley 224 programmable current source for providing current using ASTM C611-98. The voltage drop was measured by Keithley 197 autoranging digital microvoltmeter. The values reported in the text were averaged over five readings of voltage drops at different positions of the samples. EMI-SE was measured by placing the composite film (0.35 mm ± 0.05 thick) inside X-band waveguides

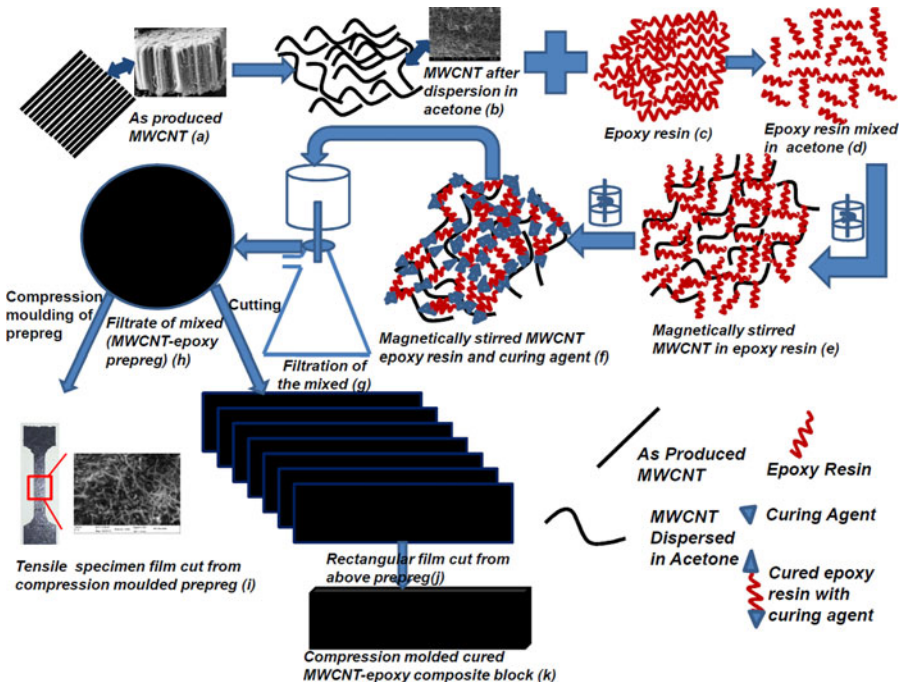

Fig. 1 Schematic diagram for preparation of high loading MWCNT–epoxy composites by filtration followed by compression molding

using a vector network analyzer (VNA) (E8263B Agilent Technologies). Magnetic measurements were performed using the vibrating sample magnetometer (VSM) model 7304 Lakeshore Cryotronics Inc., USA.

Results and discussion

Determination of weight percentage of MWCNT in composite

The weight fraction of CNT in each composite was evaluated using TGA. The TGA curves of epoxy, CNT, and composites are presented in Fig. 2. The weight loss was measured at 600 °C because thermal decomposition of MWCNT starts slightly above 600 °C. The percentages of CNTs in the epoxy obtained were 4.2, 15.1, and 20.4 wt%. The calculations were made using the method developed by Ogasawara et al. (Ogasawara et al. 2011). These were designated as CMP1, CMP2, and CMP3, respectively. Compression molded prepreg papers of CMP3 were designated as CMP4.

Mechanical properties of the composite film

Figure 3a, b show the variation in Young's modulus and tensile strength with MWCNT loading in epoxy composites. Young's modulus increased with MWCNT loading and reached up to a value of 3203 MPa (CMP3) from 1990 MPa (neat epoxy). This is due to the addition of stiffer material (CNT) into epoxy resin. The tensile strength also increased with increase in MWCNT from 42 MPa (neat epoxy) to 59 MPa (CMP3), an improvement of ~40 % over the neat polymer. The SEM micrograph of fractured surfaces of the MWCNT–epoxy composite films after

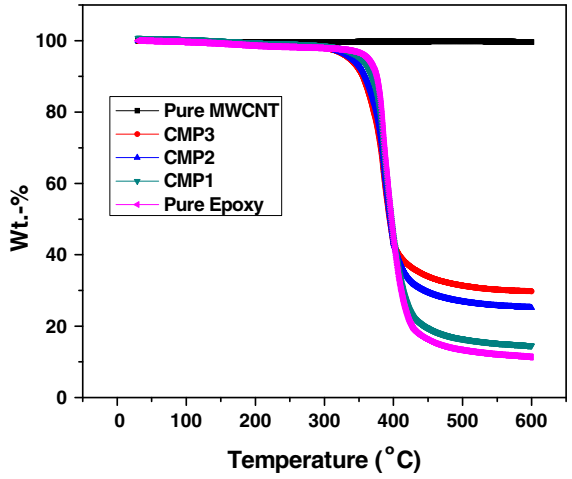

Fig. 2 Thermogravimetric analysis results of CNT, epoxy, and CNT/epoxy composites

tensile testing (Fig. 4b–d) reveal that CNTs are uniformly dispersed without any visible aggregation. Aggregation can reduce the reinforcing effect of CNTs leading to a reduction in the strength of composites. A uniform dispersion of CNTs results in good load transfer from matrix to the CNTs resulting in improved mechanical properties at high loading of CNTs. This technique of formation of CNT-dispersed epoxy composites is more effective than conventional techniques of dispersion. This technique is also different than other epoxy impregnated bucky paper based technique where epoxy resin is impregnated into bucky paper. In those techniques, proper impregnation of epoxy is very difficult due to availability of very small pores between the CNTs. In the present technique, epoxy impregnated prepreg paper is prepared by dispersing long MWCNT into epoxy resin where proper adhesion takes place between the matrix and CNTs.

Electrical conductivity of the composites

Figure 5a shows the variation of room temperature electrical conductivity with the change in MWCNT loadings. Pure epoxy is electrical insulator with d.c. electrical conductivity value of $\sim 10^{-15}$ S/cm (Barrau et al. 2003). However, conductivity of MWCNT–epoxy composites displays a systematic increase with the increase in MWCNT content from 4.2 to 20.4 wt%. The above enhancement can be attributed to the formation of extensive 3D networks of MWCNTs within epoxy matrix. In particular, the electrical conductivity is dramatically enhanced by 15 orders of magnitude for CMP1 compared to that of pristine epoxy. This can be attributed to combined effect of high aspect ratio of MWCNTs, prefect graphitic structure (interlayer spacing 0.342 nm, see HRTEM image, Fig. 5b) and its effective dispersion (Fig. 4b–d) within epoxy matrix. When the CNT loading is further increased to 20.4 wt% (CMP3), the electrical conductivity increased to 9 S/cm. The achieved conductivity value was near the prescribed range for microwave shielding. Therefore, good EMI shielding response is expected (Saini et al. 2012; Saini and Arora 2012).

Magnetization studies

Figure 6a shows the vibrating sample magnetometer (VSM) plot of CMP2, CMP3 and pure polymer whereas *inset* of Fig. 6a shows that VSM of MWCNTs and the magnetization data are presented in Table 1. It can be seen that MWCNT displays moderate ferromagnetic properties with saturation magnetization (M_s), retentivity (M_r) and coercivity (H_c) values of $\sim$7 emu/g, $\sim$2.2 emu/g, and 577 G, respectively. The observed hysteresis loop can be attributed to the presence of iron particles inside the cavity of MWCNTs as shown in the HRTEM image (Fig. 6b). It is also seen that incorporation of above MWCNTs inside non-magnetic epoxy matrix results in introduction of magnetic properties. Therefore, the M_s, M_r, and H_c values were found to be 0.79 emu/g, 0.21 emu/g, and 480 G, respectively for CMP2 and 1.33 emu/g, 0.46 emu/g, and 570 G, respectively, for CMP3. These results are of specific interest as good magnetic properties are important in modulating the shielding response (Saini et al. 2012).

EMI shielding performance

The EMI shielding is a direct consequence of reflection, absorption, and multiple internal reflection losses at the existing interfaces, suffered by incident

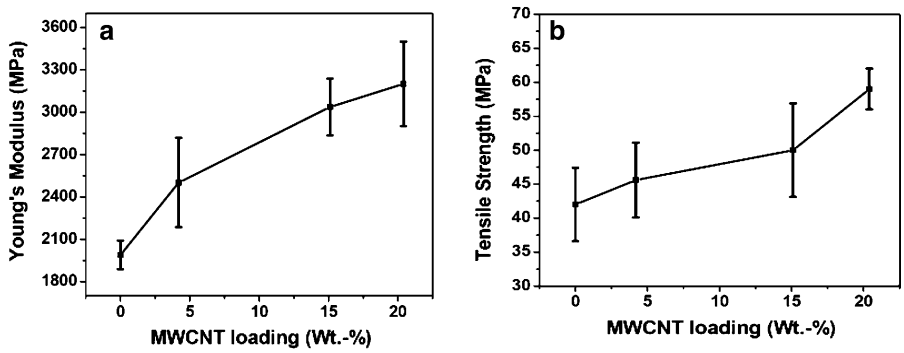

Fig. 3 Variation in **a** tensile strength and **b** Young's modulus with MWCNT loading

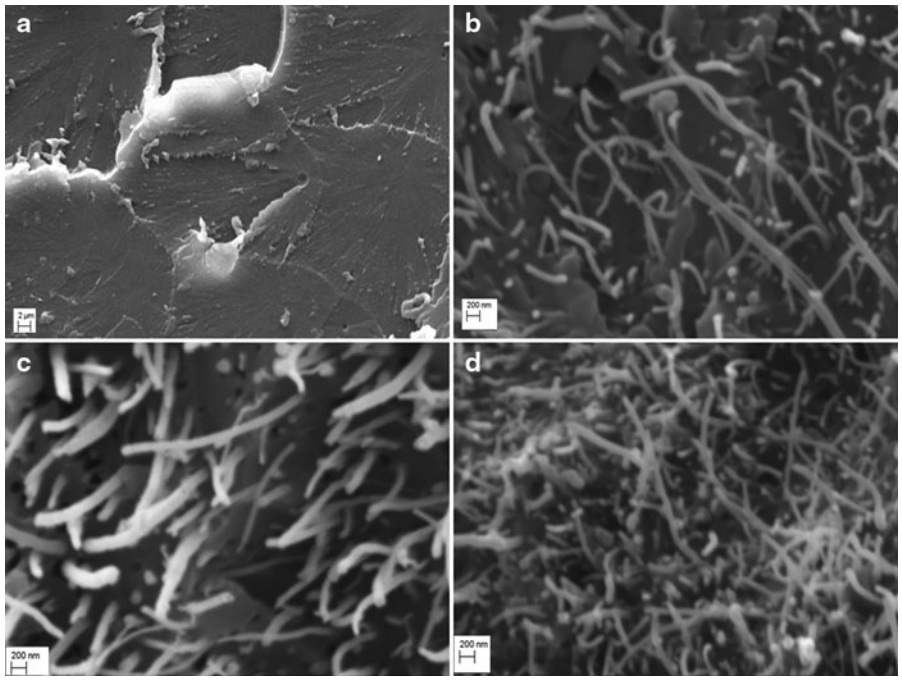

Fig. 4 Fracture surface of **a** pure epoxy, **b** 4.2 wt% MWCNT–epoxy, **c** 15.13 wt% MWCNT–epoxy and **d** 20.4 wt% MWCNT–epoxy composite film

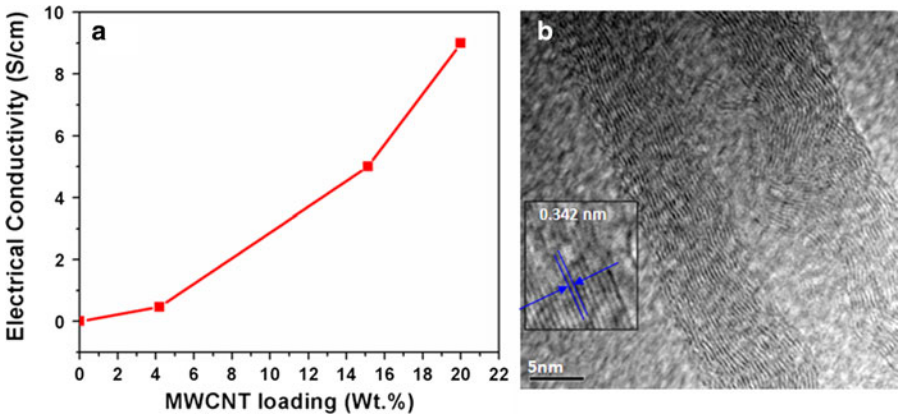

Fig. 5 **a** Variation of electrical conductivity of MWCNT–epoxy nanocomposites as a function of MWCNT content, **b** HRTEM image of individual MWCNT showing multiwall structure and well-defined lattice fringes with interplanar spacing of 0.342 nm

electromagnetic (EM) waves. The total shielding effectiveness (SE_T) can be expressed as (Saini et al. 2009; Singh et al. 2012):

$$SE_T(dB) = 10\log_{10}(P_T/P_I) = 20\log_{10}(E_T/E_I) = \log_{10}(H_T/20H_I) \quad (1)$$

where P_I (E_I or H_I) and P_T (E_T or H_T) are the power (electric or magnetic field intensity) of incident and transmitted EM waves, respectively. The scattering parameters S_{11} (S_{22}) and S_{12} (S_{21}) of VNA are related to reflectance (R) and transmittance (T), respectively, i.e., $T = |E_T/E_I|^2 = |S_{12}|^2$ ($=|S_{12}|^2$), $R = |E_R/E_I|^2 = |S_{11}|^2$ ($=|S_{22}|^2$). Therefore, attenuations due to reflection (SE_R) and absorption (SE_A) can be conveniently expressed as:

$$SE_R = 10\log_{10}(1 - R) \quad (2)$$

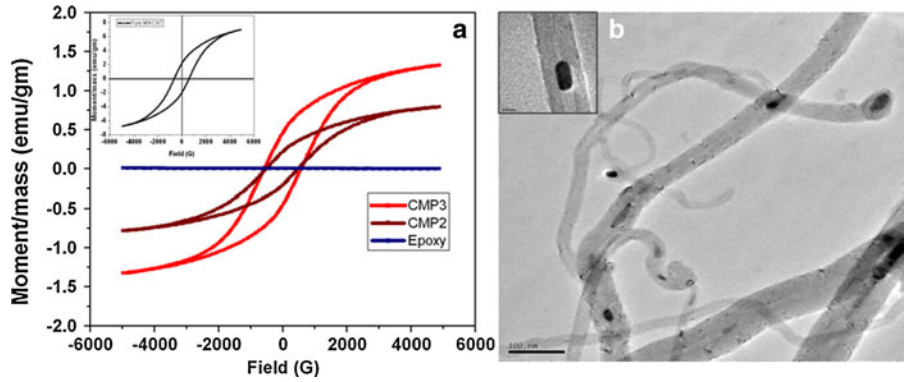

Fig. 6 **a** Magnetization studies of pure epoxy, CMP2 and CMP3 and *inset* shows for pure MWCNTs showing ferromagnetic character and hysteresis loop. **b** HRTEM image of individual MWCNT showing entrapped iron-phase within internal cavity of tubes, *inset* shows zoom-in image of entrapped iron

Table 1 Magnetization data for various samples

Sample	M_s (emu/g)	M_r (emu/g)	H_c (G)
MWCNTs	7	2.2	577
CMP2	0.79	0.21	480
CMP3	1.33	0.46	570
Pure epoxy	0.009	–	–

$$SE_A = 10\log(1 - A_{eff}) = 10\log_{10}[T/(1-R)] \quad (3)$$

Further, the angular frequency (ω) dependence of reflection and absorption losses can be expressed in the terms of total conductivity (σ_T), real permeability (μ'), skin depth (δ and thickness (t) of the shield material as (Singh et al. 2011):

$$SE_R(dB) = -10\ \log_{10}\left(\frac{\sigma_T}{16\omega\varepsilon o\mu'}\right) \quad (4)$$

$$SE_A(dB) = -20\frac{t}{\delta}\log_{10}\ e = -8.68\left(\frac{t}{\delta}\right) = -8.68t\left(\frac{\sigma_T\omega\mu'}{2}\right)^{\frac{1}{2}} \quad (5)$$

The above equations reveals that both conductivity as well as magnetic properties are useful for enhancing the absorption and hence total shielding. Therefore, use of MWCNT as conducting filler with additional magnetic properties (due to entrapped iron particles) is expected to enhance shielding effectiveness.

The shielding effectiveness value as well as electromagnetic attributes (permittivity and loss tangent) of samples is shown in Fig. 7. The results reveal that pure epoxy sample gives negligible attenuation (not shown) with ($SE_T \approx -0.3$ dB). However, with the addition of MWCNT, both reflection (SE_R) as well as absorption (SE_A) loss component increases resulting in the enhancement of total shielding (SE_T) i.e., from -10 (for CMP1) to -19 dB (CMP3) as shown in Fig. 7a. Further, the careful analysis of underlying reflection and absorption components show that SE_A/SE_R ratio (Fig. 7b) increases with incorporation of higher amount of CNTs. These results demonstrate that SE_T is dominated by absorption component, contribution of which increases with increasing MWCNT content.

The permittivity spectra of these samples show that real permittivity (dielectric constant) value decreases with increase of frequency. This can be ascribed to the inability of polarization vector to maintain in-phase movement with incident high frequency electromagnetic radiation. Further, the dielectric constant increases with loading of higher amount of CNTs which may be ascribed to the Maxwell–Wegner interfacial polarization. The large difference in the electrical conductivity of MWCNT ($\sim 10^4$ S/cm) filler and epoxy matrix (10^{-15} S/cm) resulted in charge localization at the interfaces leading to polarization and related losses. In order to explore the reason behind the enhanced absorption loss (SE_A), the dielectric loss tangent values (i.e., $\tan\delta_e = \varepsilon''/\varepsilon'$) have also been calculated which reflect the ability of a material to convert applied energy into heat. Therefore, materials with high $\tan\delta_e$ value are useful for making microwave absorbing materials in stealth technology. The results have shown that $\tan\delta_e$ increases from CMP1 to for CMP3 which is responsible for enhanced shielding response.

Figure 8a shows the magnetic permeability of the composites which shows weak frequency dependence. Furthermore, the permeability was found to increase with CNT loading which is due to the presence of iron particles within the cavity of CNT. The magnetic

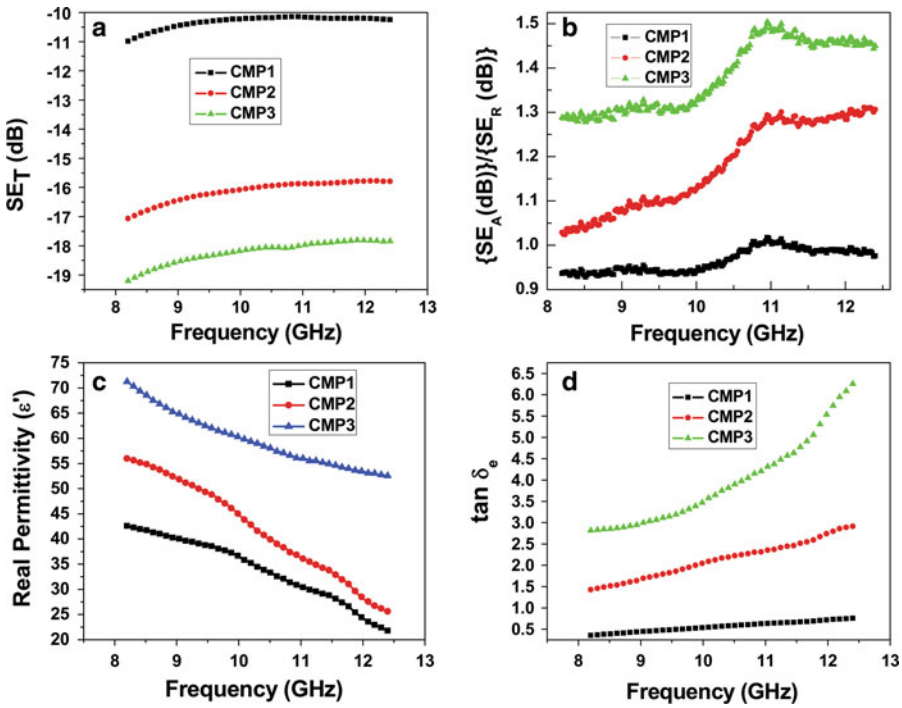

Fig. 7 Frequency dependence of **a** total shielding effectiveness (SE_T), **b** SE_A/SE_R, **c** real permittivity (ε') and **d** loss tangent ($\tan \delta_e$), for MWCNT–epoxy nanocomposites

properties help in better matching of input impedance, reduction of skin depth, and additional magnetic losses. Therefore, they contribute toward improvement of absorption loss.

The above dielectric and magnetic losses are responsible for generation of heat due to molecular friction. The safe and fast dissipation of this heat is desirable for maintaining long term and stable performance of the shield. Like other polymers, pure epoxy matrix also has very low thermal conductivity ~0.14 W/mK (Cui et al. 2011) and displays poor heat dissipation response. The addition of MWCNT with high inherent thermal conductivity ($k \sim 3000$ W/mK) leads to thermal conductivity value (Fig. 8b) of 2.175 W/mK for CMP4. Such an improvement (~15 times higher than pure epoxy) in k gives direct evidence of improvement of microwave heat dissipation characteristics of the shield. The variation in the thermal conductivity with temperature is very small (from 2.0 W/mK at 50 °C to 2.175 W/mK at 200 °C) and increases slightly with temperature. Thermal conductivity of any composite material depends mainly on the filler conductivity, dispersion, orientation, and the interfacial thermal resistance between filler and polymer. The change in thermal conductivity with temperature depends mainly on the interfacial thermal resistance which decreases with increase in temperature (Jakubinek et al. 2010). This results in

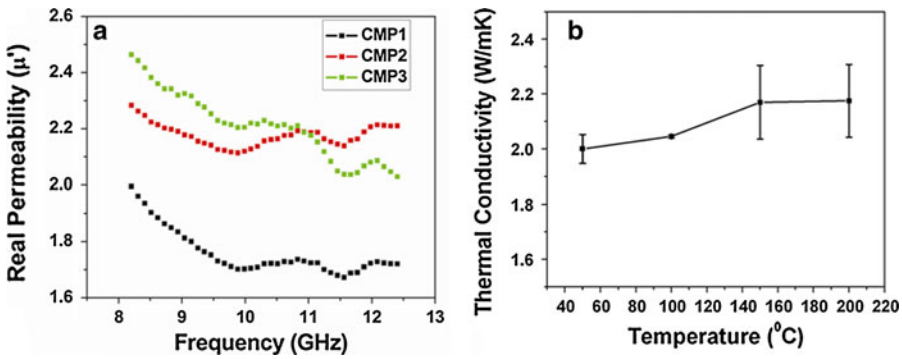

Fig. 8 **a** Frequency dependence of real magnetic permeability (μ') and **b** temperature dependence of thermal conductivity (k) of the MWCNT–epoxy shield

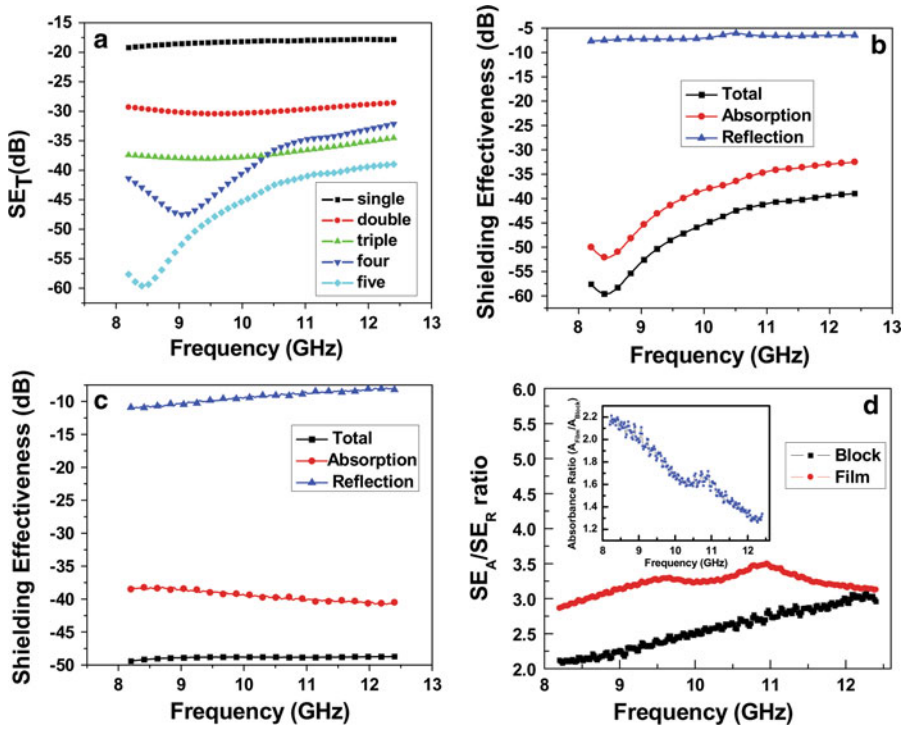

Fig. 9 Frequency dependence of **a** SE_T of CMP3 with no. of layers. **b** SE_T, SE_A, and SE_R of five layers of CMP3. **c** SE_T, SE_A, and SE_R of CMP4 of 1.75 mm thickness. **d** SE_A/SE_R for layered sample and CMP4 at 1.05 mm thickness, *inset* shows the absorption ratio of layered film vs compression molded block

Table 2 Results of shielding effectiveness of CNT based various polymer composites reported by previous authors in X-band

Type of CNT%/CNT%/thickness	Polymer	Shielding effectiveness (dB)	References
SWCNT/20 wt%/2 mm	PU	17	Liu et al. (2007)
SWCNT/15 wt%/2 mm	Epoxy	20–30	Huang et al. (2007)
MWCNT/10 vol%/0.3–2.1 mm	PMMA	18–40	Pande et al. (2009)
MWCNT/40 w%/0.165 mm	PMMA	27	Kim et al. (2004)
MWCNT/4.76 wt%/10 layers of 0.1 mm thick film	PMMA	Up to ~42	Yuen et al. (2008)
MWCNT/7 wt%/[a]	PS Foam	20	Yang and Gupta (2005)
MWCNT/5 vol%/[a]	PP	24	Al-Saleh and Sundararaj (2009)
MnO_2 nanotubes &f-MWCNTs/5 wt% MnO_2 & 1 wt% f-MWCNT/1 mm	PVDF	20	Eswaraiah et al. (2011)
MWCNT/20 wt%/1.5 mm	Styrene Acrylic Emulsion	28	Li et al. (2010)
MWCNT/40 wt%/6 mm	Cellulose Triacetate	~30	Basavaraja et al. (2011)
SWCNT/15 wt%/[a]	EVA	22–23	Das and Maiti (2008)
f-SWCNT/4.5 vol%/2 mm	RET	30	Park et al. (2010)
MWCNT/5 wt%/1.85 mm	PC	26	Arjmand et al. (2011)

[a] Thickness not mentioned

slightly higher thermal conductivity at higher temperature.

As we increase the shield thickness by stacking of layers, geometrical effects tend to come into picture and a clear loss peak is observed in the shielding curve. Moreover, as the shield thickness increases, the loss peak intensity increases and shifts toward lower frequency. This may be due to the combined effect of dielectric and magnetic properties along with geometrical (thickness) effects resulting in better matching of input impedance. Therefore, a five-layered shield with total thickness of 1.75 mm resulted in SE_T value of −60 dB at 8.3 GHz (Fig. 9a) which corresponds to blocking of more than 99.999 % of incident EM radiation. To prove further, SE_T was divided into reflection and absorption components as shown in Fig. 9b which clearly demonstrates the dominance of absorption. In order to explore the superiority of layer stacking method, a block of above composite (CMP4) with thickness of ∼1.75 mm was also prepared by compression molding. The shielding response of the block (Fig. 9c) revealed that maximum attenuation was −50 dB which was less than that observed for layered sample. Further, unlike layered sample no band was observed for bulk sample. To investigate the probable reasons, the SE_A/SE_R ratio was calculated (Fig. 9d) for a bulk and layered samples of same thickness i.e., 1.05 mm (equivalent to three layers). The results revealed that in the entire frequency range, the ratio was higher for layered sample than for its bulk counterpart. This reflected that for layered sample absorption was playing more significant role than the bulk sample. The same was also complemented by the fact that ratio of absorbance value of the film and bulk sample (*inset* Fig. 9d) was greater throughout the entire frequency range. Furthermore, reflection loss of layered sample (∼−7.0 dB, Fig. 9b) was much less than block sample (∼−10 dB, Fig. 9c) which signifies better impedance matching for the former. The better impedance matching along with higher absorption capability of the layered film sample resulted in attainment of band and higher shielding effectiveness value. The above results implied that layering is a better method of obtaining higher shielding effectiveness compared to compression molded thick block of same thickness. The observed attenuation herein crossed the limit (−30 to −40 dB) of commercial applications, which suggests that these nanocomposites are promising candidates for making futuristic radar absorbers. These results were also compared with recently conducted research on CNT–polymer composites in X-band and tabulated in Table 2. This table shows that the present result is superior to reported results.

Conclusions

MWCNT–epoxy composites were fabricated using a novel dispersion and compression molding technique which enabled dispersion of high loadings of CNTs (up to 20.4 wt%) uniformly. A value of 9 S/cm of electrical conductivity was achieved which helped in attaining high EMI shielding properties of such composites i.e., up to 60 dB in X-band which is the most desired range for commercial applications such as radar, TV picture transmission, and telephone microwave relay systems, etc. An addition of MWCNT in the epoxy also provided structural integrity to the composites with tensile strength of the order of 60 MPa along with improved thermal conductivity which is a prerequisite for efficient heat dissipation in microelectronics devices.

Acknowledgments The authors thank the Director, NPL, for his keen interest in the work. Authors would like to thank Dr. R.K.Kotnala for measurement of magnetic properties. The authors are also thankful to Mr. R.K. Seth for carrying out the TGA, Mr. K.N. Sood, and Mr. J.Tawale for carrying out SEM of the samples.

References

Allaoui A, Bai S, Cheng HM, Bai JB (2002) Mechanical and electrical properties of a MWNT/epoxy composite. Compos Sci Technol 62:1993–1998

Al-Saleh MH, Sundararaj U (2009) Electromagnetic interference shielding mechanisms of CNT/polymer composites. Carbon 47:1738–1746

Arjmand M, Mahmoodi M, Gelves GA, Park S, Sundararaj U (2011) Electrical and electromagnetic interference shielding properties of flow-induced oriented carbon nanotubes in polycarbonate. Carbon 49:3430–3440

Barrau S, Demont P, Perez E, Peigney A, Laurent C, Lacabanne C (2003) Effect of palmitic acid on the electrical conductivity of carbon nanotubes-epoxy resin composites. Macromolecules 36:9678–9680

Basavaraja C, Jo EA, Kim BS, Huh DS (2011) Electromagnetic interference shielding of cellulose triacetate/multiwalled carbon nanotube composite films. Polym Compos 32: 438–444

Cui W, Du F, Zhao J, Zhang W, Yang Y, Xie X, Mai Y-W (2011) Improving thermal conductivity while retaining high electrical resistivity of epoxy composites by incorporating silica-coated multi-walled carbon nanotubes. Carbon 49:495–500

Das NC, Maiti S (2008) Electromagnetic interference shielding of carbon nanotube/ethylene vinyl acetate composites. J Mater Sci 43:1920–1925

Eswaraiah V, Sankaranarayanan V, Ramaprabhu S (2011) Inorganic nanotubes reinforced polyvinylidene fluoride composites as low-cost electromagnetic interference shielding materials. Nanoscale Res Lett 6(137):1–11

Feng QP, Yang JP, Fu SY, Mai YW (2010) Synthesis of carbon nanotube/epoxy composite films with a high nanotube loading by a mixed-curing-agent assisted layer-by-layer method and their electrical conductivity. Carbon 48: 2057–2062

Feng QP, Shen XJ, Yang JP, Fu SY, Mai YW, Friedrich K (2011) Synthesis of epoxy composites with high carbon nanotube loading and effects of tubular and wavy morphology on composite strength and modulus. Polymer 52:6037–6045

Garg P, Singh BP, Kumar G, Gupta T, Pandey I, Seth RK, Tandon RP, Mathur RB (2011) Effect of dispersion conditions on the mechanical properties of multi-walled carbon nanotubes based epoxy resin composites. J Polym Res 18:1397–1407

Gou JH (2006) Single-walled nanotube bucky paper and nanocomposite. Polym Int 55:1283–1288

Gupta A, Choudhary V (2011) Electrical conductivity and shielding effectiveness of poly(trimethylene terephthalate)/multiwalled carbon nanotube composites. J Mater Sci 46:6416–6423

Huang Y, Li N, Ma Y, Feng D, Li F, He X, Lin X, Gao H, Chen Y (2007) The influence of single-walled carbon nanotube structure on the electromagnetic interference shielding efficiency of its epoxy composites. Carbon 45:1614–1621

Jakubinek MB, White MA, Mu M, Winey KI (2010) Temperature dependence of thermal conductivity enhancement in single-walled carbon nanotube/polystyrene composites. App Phys Lett 96:083105-1-3

Kim HM, Kim K, Lee CY, Joo J, Cho SJ, Yoon HS, Pejakovic DA, Yoo JW, Epstein AJ (2004) Electrical conductivity and electromagnetic interference shielding of multiwalled carbon nanotube composites containing Fe catalyst. Appl Phys Lett 84:589–591

Li N, Huang Y, Du F, He XB, Lin X, Gao HJ, Ma YF, Li FF, Chen YS, Eklund PC (2006) Electromagnetic interference (EMI) shielding of single-walled carbon nanotube epoxy composites. Nano Lett 6:1141–1145

Li Y, Chen C, Zhang S, Ni Y, Huang J (2008) Electrical conductivity and electromagnetic interference shielding characteristics of multiwalled carbon nanotube filled polyacrylate composite films. Appl Surf Sci 254:5766–5771

Li Y, Chen C, Li J-T, Zhang S, Ni Y, Cai S, Huang J (2010) Enhanced dielectric constant for efficient electromagnetic shielding based on carbon-nanotube-added styrene acrylic emulsion based composite. Nanoscale Res Lett 5:1170–1176

Liu Z, Bai G, Huang Y, Ma Y, Du F, Li F, Guo T, Chen Y (2007) Reflection and absorption contributions to the electromagnetic interference shielding of single-walled carbon nanotube/polyurethane composites. Carbon 45:821–827

Mathur RB, Chatterjee S, Singh BP (2008a) Growth of carbon nanotubes on carbon fibre substrates to produce hybrid/phenolic composites with improved mechanical properties. Compos Sci Technol 68:1608–1615

Mathur RB, Pande S, Singh BP, Dhami TL (2008b) Electrical and mechanical properties of multi-walled carbon nanotubes reinforced PMMA and PS composites. Polym Compos 29:717–727

Morais WA DDaJ, Godfroid LB (2003) Effect of the fiber reinforcement on the low energy impact behaviour of fabric reinforced resin matrix composite materials. J Braz Soc Mech Sci Eng 25:325–328

Ogasawara T, Moon SY, Inoue Y, Shimamura Y (2011) Mechanical properties of aligned multi-walled carbon nanotube/epoxy composites processed using a hot-melt prepreg method. Compos Sci Technol 71:1826–1833

Pande S, Singh BP, Mathur RB, Dhami TL, Saini P, Dhawan SK (2009) Improved electromagnetic interference shielding properties of MWCNT-PMMA composites using layered structures. Nanoscale Res Lett 4:327–334

Park JG, Louis J, Cheng QF, Bao JW, Smithyman J, Liang R, Wang B, Zhang C, Brooks JS, Kramer L, Fanchasis P, Dorough D (2009) Electromagnetic interference shielding properties of carbon nanotube buckypaper composites. Nanotechnology 20:415702–415708

Park S-H, Theilmann PT, Asbeck PM, Bandaru PR (2010) Enhanced electromagnetic interference shielding through the use of functionalized carbon-nanotube-reactive polymer composites. IEEE Trans Nanotechnol 9:464–469

Saini P, Arora M (2012) In: Gomes AD (ed) New polymers for special applications. Intech, Croatia, doi:10.5772/48779; http://www.intechopen.com/download/pdf/38964

Saini P, Choudhary V, Singh BP, Mathur RB, Dhawan SK (2009) Polyaniline-MWCNT nanocomposites for microwave absorption and EMI shielding. Mater Chem Phys 113:919–926

Saini P, Choudhary V, Singh BP, Mathur RB, Dhawan SK (2011) Enhanced microwave absorption behavior of polyaniline-CNT/polystyrene blend in 12.4-18.0 GHz range. Synth Met 161:1522–1526

Saini P, Choudhary V, Vijayan N, Kotnala RK (2012) Improved electromagnetic interference shielding response of poly (aniline)-coated fabrics containing dielectric and magnetic nanoparticles. J Phys Chem C 116:13403–13412

Singh BP, Singh D, Mathur RB, Dhami TL (2008) Influence of surface modified MWCNTs on the mechanical, electrical and thermal properties of polyimide nanocomposites. Nanoscale Res Lett 3:444–453

Singh BP, Prabha Saini P, Gupta T, Garg P, Kumar G, Pande I, Pande S, Seth RK, Dhawan SK, Mathur RB (2011) Designing of multiwalled carbon nanotubes reinforced low density polyethylene nanocomposites for suppression of electromagnetic radiation. J Nanopart Res 13:7065–7074

Singh BP, Choudhary V, Saini P, Mathur RB (2012) Designing of epoxy composites reinforced with carbon nanotubes grown carbon fiber fabric for improved electromagnetic interference shielding. AIP Adv 2:022151

Wang Z, Liang ZY, Wang B, Zhang C, Kramer L (2004) Processing and property investigation of single-walled carbon

nanotube (SWNT) buckypaper/epoxy resin matrix nanocomposites. Compos A Appl Sci Manuf 35:1225–1232

Wardle BL, Saito DS, Garcia EJ, Hart AJ, de Villoria RG, Verploegen EA (2008) Fabrication and characterization of ultrahigh-volume-fraction aligned carbon nanotube-polymer composites. Adv Mater 20:2707–2714

Yang YL, Gupta MC (2005) Novel carbon nanotube-polystyrene foam composites for electromagnetic interference shielding. Nano Lett 5:2131–2134

Yang K, Gu MY, Guo YP, Pan XF, Mu GH (2009) Effects of carbon nanotube functionalization on the mechanical and thermal properties of epoxy composites. Carbon 47:1723–1737

Yuen S-M, Ma C-CM, Chuang C-Y, Yu K-C, Wu S-Y, Yang C–C, Wei M-H (2008) Effect of processing method on the shielding effectiveness of electromagnetic interference of MWCNT/PMMA composites. Compos Sci Technol 68: 963–968